Available online at www.sciencedirect.com
SCIENCE DIRECT®
Ultramicroscopy 105 (2005) 324–329
ultramicroscopy
www.elsevier.com/locate/ultramic

Development of a shear force scanning near-field fluorescence microscope for biological applications

G.Y. Shang[a], W.H. Qiao[b], F.H. Lei[a,b], J.-F. Angiboust[b], M. Troyon[a,*], M. Manfait[b]

[a]*LMEN, (EA), UFR des Sciences, Université de Reims Champagne-Ardenne, 21 rue Clément Ader, 51685 Reims Cédex 2, France*
[b]*Unité MéDIAN, CNRS-UMR 6142, UFR de Pharmacie, IFR 53, Université de Reims Champagne-Ardenne, 51 rue Cognacq Jay, 51096 Reims Cédex, France*

Received 2 July 2004; received in revised form 8 May 2005

Abstract

In this paper, a shear force scanning near-field fluorescence microscope combined with a confocal laser microspectrofluorometer is described. The shear force detection is realized based on a bimorph cantilever, which provides a very sensitive, reliable, and easy to use method to control the probe–sample distance during scanning. With the system, high-quality shear force imaging of various samples has been carried out. Furthermore, simultaneous shear force and near-field fluorescence imaging of biological cells has also been realized. As an example, we especially present the result on the distribution of P-glycoprotein in the plasma membrane of human small cell lung cancer cells, suggesting that the system would be a promising tool for biological applications.

PACS: 07.79.−v; 07.79.Fc

Keywords: Shear force; Near-field fluorescence; Biological cell

1. Introduction

Although scanning near-field optical microscopy (SNOM) [1–3] has been regarded as a promising method for the study of biological systems, it is not easy to effectively apply SNOM to problems of practical interest, in particular, biological cells. The fact is that there have been a few reports on biological cell investigation [4–7]. The main difficulties in performing near-field imaging of cells would include: (i) the difficulty in keeping the probe at a fixed relative distance from a cell surface while imaging, (ii) the need for a relatively large scan range in *z*-axis, (iii) the

*Corresponding author. Tel.: +33 32605 1901; fax: +33 32605 1900.
E-mail address: michel.troyon@univ-reims.fr (M. Troyon).

0304-3991/$ - see front matter © 2005 Elsevier B.V. All rights reserved.
doi:10.1016/j.ultramic.2005.06.044

necessity to position the probe on a particular cell from tens or hundreds of cells, and (iv) very low fluorescence intensity.

Based on the bimorph cantilever method [8,9], we have developed a shear force scanning near-field fluorescence microscope (ShF-SNFM), which is designed to be able to combine with a confocal laser microspectrofluorometer (CLMF) for overcoming the above difficulties. After describing the main parts of the system and the result on shear force imaging in this paper, we especially focus on demonstrating it for biological applications: the distribution of P-glycoprotein in the plasma membrane of human small cell lung cancer cells investigated with the system will be presented.

2. Instrumentation

2.1. CLMF

The CLMF consists of an inverted optical microscope (Olympus IX70, Japan), a confocal optical system and a spectrofluorometer (Micro-Fluo, Jobin-Yvon, France), equipped with a two-dimensional liquid nitrogen CCD detector (Spectrum ONE CCD2000, USA) and an argon ion laser (Spectra Physics, USA). In the CLMF, light emitted from the argon ion laser is focused on a certain point in a sample through the confocal system and the inverted optical microscope. The same point is subsequently imaged on the CCD detector through the same optics and an optical fiber cable. Using a high numerical aperture objective lens, the lateral intensity distribution in the sample is limited to sub-micrometer. The intensity distribution on the optical axis is restricted by using an adjustable detection pinhole in the image plane resulting in the spatial suppression of out-of-focus signal. The spectrofluorometer allows one to acquire fluorescence radiation spectra from the point in the sample.

2.2. ShF-SNFM setup

The ShF-SNFM setup is designed to mount on the sample stage of the inverted optical microscope, and its central part is schematically shown in Fig. 1. A piezoelectric bimorph cantilever perpendicular to the sample surface is rigidly clamped at its upper end and an optical fiber probe is attached to one side. For shear force detection, the middle electrode of the bimorph is grounded. The left (or right) piezolayer, serving as a dither piezo, is connected to a reference signal generator of the lock-in amplifier. When applying a constant sine wave voltage to the dither piezo, mechanical vibration of the cantilever takes place due to the anti-piezoelectric effect. Meanwhile, the right (or left) piezolayer generates an induced piezovoltage originating from piezoelectric effect. Consequently, as the cantilever is driven at its resonance frequency by the dither piezo, the detection piezo generates a maximum piezo voltage. The voltage is detected by a preamplifier, then demodulated by the lock-in, and finally used for probe–sample distance control. A flat scanner (Nis-50, Nanonics Imaging Ltd.) is equipped since it has the unique advantage of small size in the vertical direction, allowing the setup to be combined with the inverted optical microscope. For positioning the probe on an interesting area, movement of the sample is carried out based on the slip-stick mechanism [10]. The whole system is mounted on a vibration isolation table.

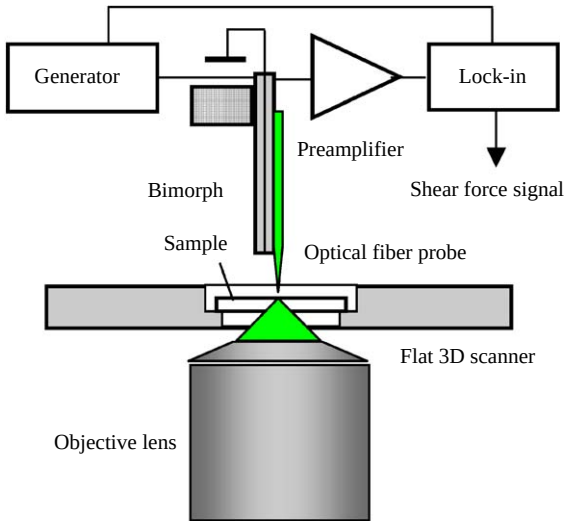

Fig. 1. Schematic of the SNFM setup mounted on the inverted optical microscope.

Fluorescence emission from a sample can be excited by the argon laser light through the optics of the CLMF and collected by the optical fiber probe, or through the optical fiber probe and collected by the CLMF optics. A photomultiplier tube (PMT, R4220P, Hamamatsu, Japan), specially selected for both high sensitivity and low dark current, is used to detect fluorescence signal. A high-pass filter with an extinction coefficient of 10^{-5} is introduced to remove the exciting light.

2.3. Electronic system

A commercially available SPM controller (NT-MDT Co.) is used, which provides the abilities of reference signal generation, lock-in measurement, feedback control, x–y scan, and data acquisition. A preamplifier (Keithley, 610C, USA) is employed to detect the photocurrent from the PMT.

3. Results and discussion

3.1. Shear force imaging

The performance of the system is first characterized by shear force imaging of various specimens including semiconductor, polymer, and biological cells. Fig. 2 shows a typical image of a close-packed layer of polystyrene spheres, obtained at the setpoint ~0.96 of the maximum vibration amplitude and the line scan frequency of 0.3 Hz. The specimen was prepared by spin coating on a freshly cleaved mica substrate. A high-resolution imaging is achieved with the system, since the contour of each sphere can be clearly resolved. A cross-section profile along the line A–B marked in Fig. 2(a) is given in Fig. 2(b), indicating that the probe perfectly tracks the sample surface without an evidence of the sphere deformation.

3.2. Shear force and near-field fluorescence imaging

With the system, the distribution of P-glycoprotein (P-gp) in the plasma membrane of human small cell lung cancer cells (H69/VP) [11] was investigated. P-gp is a transmembrane glycoprotein with a molecular weight of 170 kDa, which is expressed in various multi-drug resistance (MDR) cells [12,13]. MDR is one type of drug resistance, presenting a major obstacle to the successful treatment of cancer [14,15]. In the present measurement, P-gp is specifically labeled with

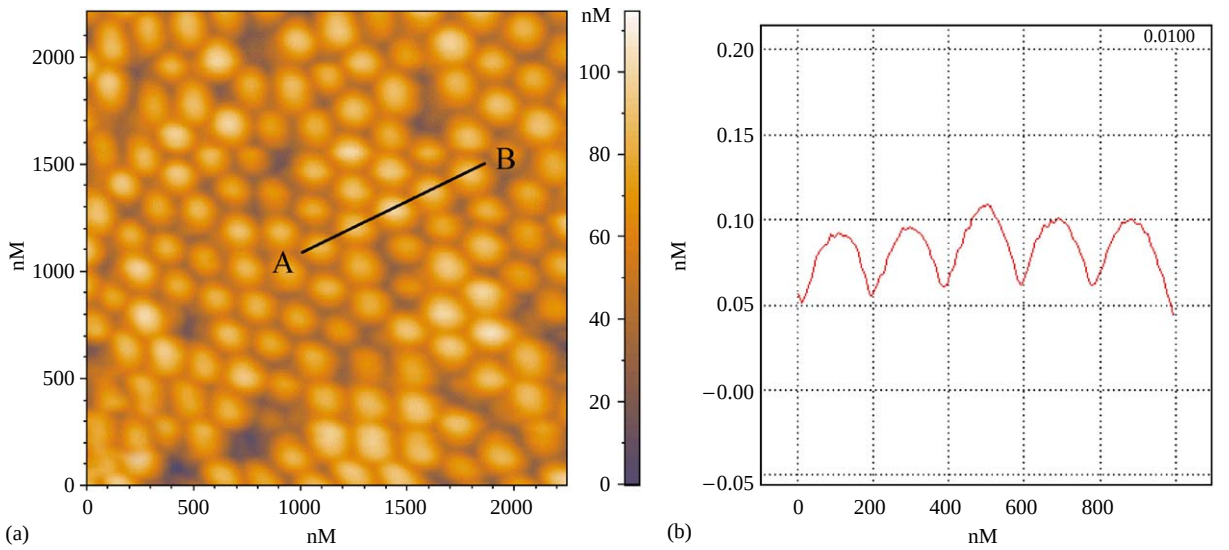

Fig. 2. (a) Shear force topographic image of a close-packed layer of polystyrene spheres on a freshly cleaved mica substrate. (b) Cross-section profile along the line A–B marked in Fig. 2(a).

monoclonal antibody UIC_2 and then stained with fluorescent dye Texas red. The sample preparation will be described in detail in a separate paper.

Shear force topographic and near-field fluorescence images of the H69/VP cancer cells were simultaneously obtained and typical results are shown in Fig. 3, taken at the setpoint of 0.96 and line scan frequency ~0.1 Hz. In the topographic image shown in Fig. 3(a), the whole shape of a single cell is presented. The corresponding near-field fluorescence image in Fig. 3(b) is very different from the shear force topographic one. As mentioned above, the P-gp has been specifically labeled with monoclonal antibody UIC_2 and then stained with fluorescent dye Texas red. Since the fluorescence intensity depends mainly on the amount of fluorescent dye, the distribution of the fluorescence intensity represents the distribution of

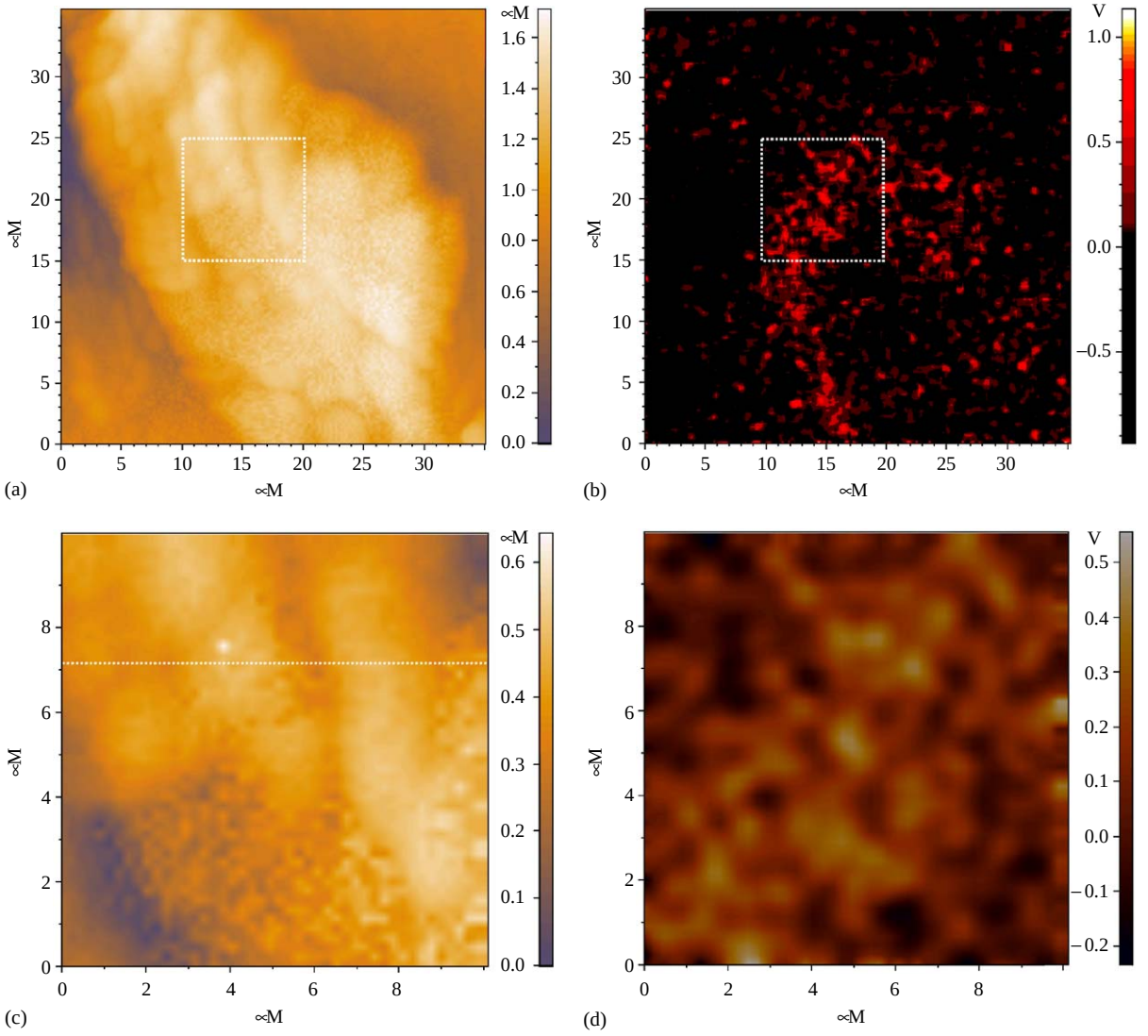

Fig. 3. (a) Shear force topographic and (b) corresponding near-field fluorescence images of a single H69/VP cancer cell stained with Texas red dye. (c) Topographic and (d) fluorescence images of the rectangular area shown in images (a) and (b), respectively.

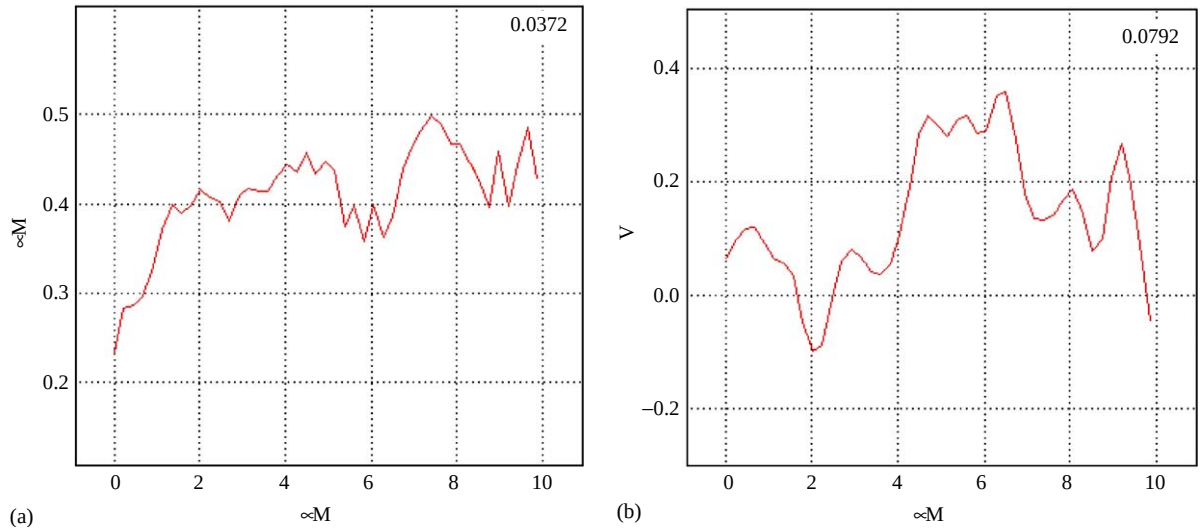

Fig. 4. (a) Topographic and (b) optical line profiles extracted at the position indicated by the line in Fig. 3(c).

P-gp in the plasma membrane of the cell. A region containing a larger amount of P-gp should exhibit higher fluorescence intensity than that containing a less amount of P-gp.

What is important is the comparison between topography and fluorescence images of the cell to analyze the distribution of P-gp in the cell membrane. In the topography, the whole shape of the cell can be seen. In the fluorescence image, a ring-like region with high fluorescence intensity is appearing around the central area of the cell, indicating that this ring-like region might have a high P-gp density and the distribution of P-gp in the cell membrane is not homogeneous.

Furthermore, some fine structures on the cell surface, including small holes and granules with minimum sizes of about 200 nm, can be resolved in Fig. 3(c). Numerous studies have provided evidence for the existence of distinct domains in the sub-micrometer range in the plasma membrane [6,16]. Although it is not sure that those structures could be attributed to domains existing in the plasma membrane of the cell for the present experiment, our system would provide an alternative way for further study of structures in the cell membrane in sub-micrometer scale. From the fluorescence image shown in Fig. 3(d), the fluorescence intensity appearing in a form of clusters can be clearly observed, the minimum size of which is ~600 nm. Since the fluorescence intensity is determined by the amount of P-gp or the complex of P-gp–antibody–Texas red, it would be concluded that P-gp forms clusters in the plasma membrane of H69/VP cells. Cluster formation may be a general property of P-gp, and the cluster of P-gp may play an important role in MDR. Of course, in order to reconfirm these results, investigations and studies should be performed further.

Finally, it should be pointed out that the near-field fluorescence image is not an artifact of the sample topology, because the feature of the fluorescence image is independent of the topographic one. This fact is better described in Fig. 4, where two line profiles extracted from the data of Figs. 3(c) and (d) are plotted, respectively. The difference between topography and fluorescence signal is evident, indicating that the two signals are not directly related. The resolution is also different between them. Edge resolution, defined as the lateral displacement with a change from 10% to 90% of the vertical variation, is estimated to be smaller than 200 nm for the topographic image. The optical resolution is a little worse, about

250 nm, i.e., $\lambda/2.5$ for the fluorescence emission peak ($\lambda\sim620$ nm).

4. Conclusions

We have successfully developed a shear force scanning near-field fluorescence microscope (ShF-SNFM), which can be combined with a confocal laser microspectrofluorometer (CLMF). Probe–-sample distance control, which is a key technique in this system, is realized based on a non-optical force sensing method. The main characteristic of the method is the use of a bimorph cantilever, which carries out simultaneous excitation and detection of mechanical vibration at its resonance frequency due to piezoelectric and anti-piezoelectric effects, leading to simplicity, compactness, and easy implementation. Moreover, the performance of the method is tested and the results show that it is very reliable and sensitive to regulate the probe–sample distance while imaging.

Application directed towards biological cells is demonstrated. As an example, the distribution of P-gp in the plasma membrane of human small cell lung cancer cells is investigated with sub-diffraction resolution. The distribution of P-gp is found to be not homogeneous and cluster formation of P-gp is observed. These results suggest that the system would be a promising tool for biological applications and provide valuable informatio for understanding some biological problems.

References

[1] D.W. Pohl, W. Denk, M. Lanz, Appl. Phys. Lett. 44 (1984) 651.
[2] E. Betzig, P.L. Finn, J.S. Weiner, Appl. Phys. Lett. 60 (1992) 2484.
[3] R. Toledo-Crow, P.C. Yang, Y. Chen, M. Vaez-Iravani, Appl. Phys. Lett. 60 (1992) 2957.
[4] Eiichi Tamiya, Shinichiro Iwabuchi, Naoki Nagatani, Yuji Murakami, Toshifumi Sakaguchi, Kenji Yokoyama, Anal. Chem. 69 (1997) 3697.
[5] Th. Enderle, T. Ha, D.S. Chemla, S. Weiss, Ultramicroscopy 71 (1998) 303.
[6] P. Nagy, A. Jenei, A.K. Kirsch, J. Szöllösi, S. Damjanovich, T.M. Jovin, J. Cell Sci. 112 (1999) 1733.
[7] A. Cricenti, R. Generosi, M. Luce, P. Perfetti, G. Margaritondo, D. Talley, M.A. Rizzo, D.W. Piston, Biophys. J. 85 (2003) 2705.
[8] G.Y. Shang, C. Wang, J. Wu, C.L. Bai, F.H. Lei, Rev. Sci. Instrum. 72 (2001) 2344.
[9] G.H. Shang, F.H. Lei, M. Troyon, W.H. Qiao, A. Trussardi-Regnier, M. Manfait, J. Microsc. 215 (2004) 127.
[10] Ch. Renner, Ph. Niedermann, A.D. Kent, Ø. Fischer, Rev. Sci. Instrum. 61 (1990) 965.
[11] I. Brock, R.D.R. Hipfner, B.S. Nielsen, P.B. Jensen, R.G. Deeley, S.P.C. Cole, M. Sehested, Cancer Res. 55 (1995) 459 (The sample was kindly supplied by Prof. M. Sehested, Denmark).
[12] K.-V. Chin, I. Pastan, M.M. Gottesman, Adv.Cancer Res. 60 (1993) 157.
[13] D.W. Loe, R.G. Deeley, S.P.C. Cole, J. Cancer 32A (1996) 945.
[14] J.L. Biedler, Cancer Res. 54 (1994) 666.
[15] J.L. Biedler, H. Riehm, Cancer Res. 30 (1970) 1174.
[16] J. Hwang, L.A. Gheber, L. Margolis, M. Edidin, Biophys. J. 74 (1998) 2184.